Journal of Contaminant Hydrology 175-176 (2015) 60–71

Contents lists available at ScienceDirect

Journal of Contaminant Hydrology

journal homepage: www.elsevier.com/locate/jconhyd

Short and long term release mechanisms of arsenic, selenium and boron from a tunnel-excavated sedimentary rock under in situ conditions

Shuichi Tamoto [a,b], Carlito Baltazar Tabelin [b,*], Toshifumi Igarashi [b], Mayumi Ito [b], Naoki Hiroyoshi [b]

[a] Civil Engineering Research Institute for Cold Region, Public Works Research Institute, Sapporo, Japan
[b] Division of Sustainable Resources Engineering, Faculty of Engineering, Hokkaido University, Sapporo, Japan

ARTICLE INFO

Article history:
Received 18 June 2014
Received in revised form 12 December 2014
Accepted 20 January 2015
Available online 29 January 2015

Keywords:
Arsenic
Boron
Selenium
Sedimentary rock
Leaching
In situ column experiments

ABSTRACT

Sedimentary rocks of marine origin excavated from tunnel construction projects usually contain background levels of hazardous trace elements, but when exposed to the environment, they generate leachates with concentrations of arsenic (As), selenium (Se) and boron (B) exceeding the WHO guideline for drinking water. In this study, the leaching of As, Se and B was evaluated under in situ conditions at various flow patterns, particle size distributions and column thicknesses. The results showed that these trace elements were leached out of the rock via short and long term mechanisms. In the short term, all three elements were rapidly and simultaneously released due to the dissolution of soluble evaporite salts formed from entrapped sea water of the Cretaceous. After their rapid release, however, these trace elements behaved differently as a result of their contrasting adsorption affinities onto minerals like clays and Fe-oxyhydroxides, which were further influenced by the pH, presence of coexisting ions and speciation of the trace elements. Selenium was quickly and easily transported out of the columns because it was mostly present as the very mobile selenate ion (Se[VI]). In comparison, the migration of As and B was hindered by adsorption reactions onto mineral phases of the rock. Boron was initially the least mobile among the three because of its preferential adsorption onto clay minerals that was further enhanced by the slightly alkaline pH and high concentrations of Ca^{2+} and Na^{+}. However, it was gradually re-mobilized in the latter part of the experiments because it was only weakly adsorbed via outer sphere complexation reactions. In the long term, the rock continued to release substantial amounts of As, Se and B via pyrite oxidation and adsorption/desorption reactions, which were regulated by the temperature and rainfall intensity/frequency on site.

1. Introduction

Arsenic (As), selenium (Se) and boron (B) are among the most common and persistent trace inorganic contaminants in the environment that are strictly regulated because of their dose-dependent toxicities. Arsenic is well-known for its lethal and carcinogenic properties (Cebrian et al., 1983; Chakraborty and Saha, 1987; Chen et al., 1985, 1992; Smith et al., 1992) while Se and B, though essential micronutrients, are toxic at high concentrations. Selenium is a key component of glutathione peroxidases, enzymes vital in the metabolism and detoxification of oxygen, while B is essential during calcium metabolism and utilization (Levander et al., 1983; Navarro-Alarcon and Cabrera-Vique, 2008; Nève, 1991; Rotruck et al., 1973). In controlled dosages, Se and B also have important

* Corresponding author. Tel./fax: +81 11 706 6315.
E-mail addresses: 95353@ceri.go.jp (S. Tamoto), carlito@eng.hokudai.ac.jp (C.B. Tabelin), tosifumi@eng.hokudai.ac.jp (T. Igarashi), itomayu@eng.hokudai.ac.jp (M. Ito), hiroyosi@eng.hokudai.ac.jp (N. Hiroyoshi).

http://dx.doi.org/10.1016/j.jconhyd.2015.01.003
0169-7722/

medicinal uses. Selenium is used to reduce heavy metals and xenobiotic toxicity (Ganther, 1980), prevent the endemic fatal cardiomyopathy called "Keshan" disease (Yang et al., 1983), and treat muscular dystrophy appearing in patients on long-term parenteral nutrition (Van Rij et al., 1979). Likewise, B prevents and treats various forms of arthritis, as well as improves psychomotor response, brain function and estrogen ingestion response in postmenopausal women (Havercroft and Ward, 1991; Nielsen, 1994; Nielsen et al., 1987, 1990; Shah and Vohora, 1990; Travers et al., 1990). In excess, however, Se increases the risks of developing breast, colorectal and kidney cancers, melanoma and lymphoid neoplasms, Parkinson's disease, and amyotrophic lateral sclerosis (ALS) (Ayaz et al., 2008; Brtko and Filipcik, 1994; Chatterjee and Banerjee, 1982; Maraldi et al., 2011; Stoica et al., 2000; Vinceti et al., 1995, 1996, 1998, 2013) while B causes nausea, vomiting, diarrhea, abdominal cramps, erythematous lesions on the skin and mucous membranes, circulatory collapse, tachycardia, cyanosis, delirium, convulsions, and coma (Beyer et al., 1983; Siegel and Wason, 1986).

Hazardous trace elements are sometimes naturally concentrated in rocks, soils and sediments as a result of certain geological processes and anomalies. One such process is the hydrothermal alteration of rocks, which occurs when rocks and solute-rich superheated solutions/fluids interact with each other. This process transforms ordinary rocks into hydrothermally altered rocks enriched with As and heavy metals (Pirajno, 2009; Tabelin et al., 2012b). Hydrothermal alteration of rocks is a widely studied topic because of its importance in the formation of precious and base metallic ores. On an environmental perspective, however, such rocks are hazardous and potential sources of toxic inorganic contaminants. In our previous studies, we conducted batch, column and in situ experiments to understand the leaching behavior and release mechanisms of several trace elements (e.g., As and lead (Pb)) contained in such rocks as well as proposed ways of mitigating their negative impacts to the environment (Tabelin and Igarashi, 2009; Tabelin et al., 2010; Tabelin et al., 2012a, 2012b, 2012c; Tatsuhara et al., 2012; Tabelin et al., 2013; Tabelin et al., 2014a).

More recently, we have identified marine sedimentary rocks as another naturally occurring material that are potential sources of hazardous trace contaminants. Although marine sedimentary rocks generally have low concentrations of trace elements (i.e., close to background levels), they are capable of generating leachates with concentrations of hazardous trace elements (e.g., As, Se and B) exceeding the environmental standards of Japan and the WHO guideline for drinking water (Tabelin et al., 2014b,2014c). These results were quite disturbing given the facts that sedimentary rocks are widespread in nature and make up a significant portion of most aquifer systems. Numerous studies have been conducted on sedimentary rocks especially those pertaining to their diagenesis, stratigraphy, mineralogical composition and physical properties (Bjørlykke, 2013; Prezbindowski and Tapp, 1991), but hardly any have been done to understand how hazardous trace elements behave when these rocks are exposed to the environment.

In our previous studies, we reported that the leaching behaviors of As, Se and B in marine sedimentary rocks largely depended on the stability of minerals/phases containing the bulk of these elements (i.e., solid-phase partitioning) and the pH of the rock–water system (Tabelin et al., 2014b,2014c). The mobilities of As and Se, for instance, were regulated by processes like dissolution of soluble phases, adsorption/desorption and pyrite oxidation, the extents of which varied depending on the pH of the rock–water system (Tabelin et al., 2014c). These previous studies, though insightful, were done using batch reactor-type experiments whose results do not provide much about how trace elements behave with variations in temperature, rainfall, infiltration rate and water content. Such variations are prevalent in the actual field setting and essential for the appropriate management of these rocks.

To address these issues, we conducted column experiments under in situ conditions for 821 days. In these experiments, we evaluated how water saturation/content, particle size distribution and rock bed thickness affected the leaching of As, Se and B from a sedimentary rock sample of marine origin. Throughout the in situ experiments, we continuously monitored changes in temperature, volumetric water content (θ), partial pressure of oxygen (PO_2) and electrical conductivity (EC) within the columns as well as the evolutions of As, Se, B and coexisting ions in the effluents. Furthermore, geochemical modeling was used to predict the speciation of trace elements and provide insights into the stability of mineral phases/constituents of the rock (e.g., Fe-oxyhydroxides and clay minerals).

2. Materials and methods

2.1. Sedimentary rock of marine origin

The sedimentary rock sample used in this study was a mixture of mudstone and sandstone formed during the Cretaceous. It was collected from the interim storage area of a road-tunnel project in northern Hokkaido, Japan. The chemical and mineralogical properties including the solid-phase partitioning of As, Se and B in this rock were reported in our previous studies (Tabelin et al., 2014b, 2014c). Quartz and plagioclase are the main mineral components of this rock (Supplementary Fig. 1). Calcite, chlorite and mica were also detected in minor quantities while pyrite was found in trace amounts. This rock contains 9, 0.59 and 113 mg/kg of As, Se and B, respectively (Tabelin et al., 2014b), which are all within the reported average concentration ranges of these elements in sedimentary rocks and soils (Fishbein, 1983; Girling, 1984; Ishikawa and Nakamura, 1993; Spears, 1964; Webster, 1999). The majority of As and Se in this rock was partitioned with the exchangeable (As: 3.1 mg/kg; Se: 0.24 mg/kg) and sulfide phases (As: 3.4 mg/kg; Se: 0.15 mg/kg) (Tabelin et al., 2014c). In comparison, B was mostly associated with the refractory crystalline/residual phase (75 mg/kg). However, amounts of this element partitioned with the exchangeable (18 mg/kg) and carbonate (9.3 mg/kg) phases were still significant.

2.2. Column experiments

2.2.1. Apparatus

The in situ column setup used in this study is illustrated in Fig. 1. The cylindrical tubes are made of PVC with an inner diameter of 298 mm and a height of 780 mm. They were mounted on an insulated-steel box bolted on a solid concrete slab. After construction of the columns, fine-meshed PVC

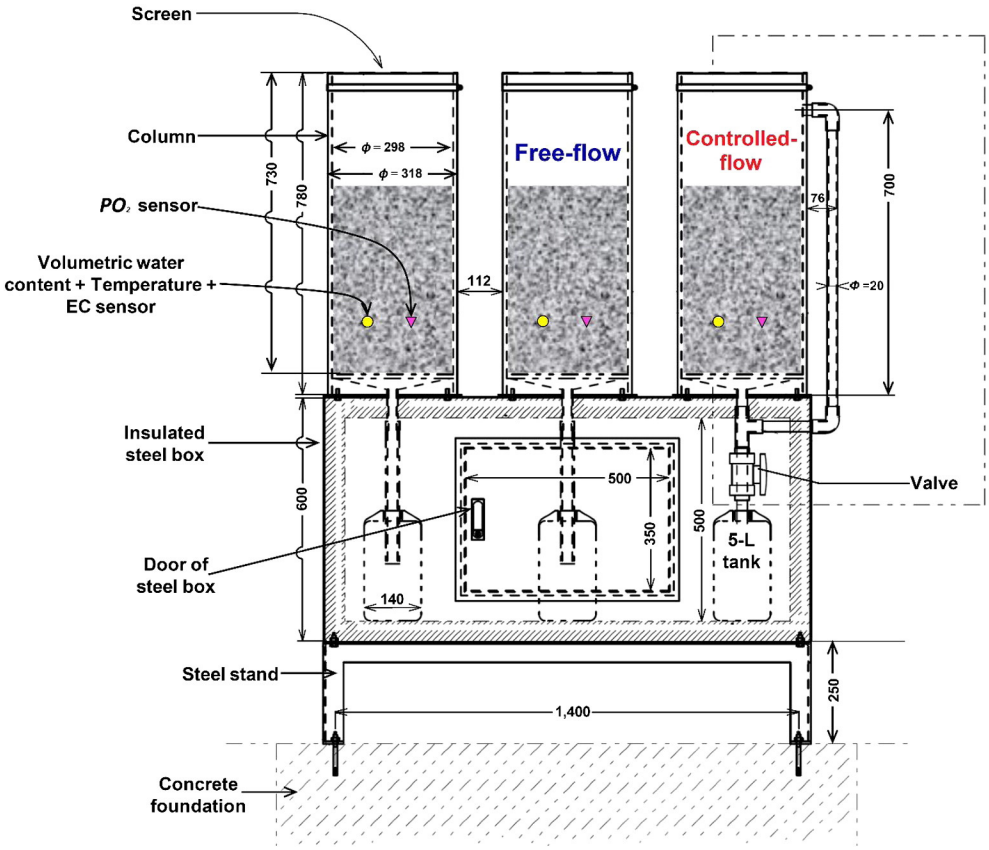

Fig. 1. Schematic diagram of the in situ column experimental setup. Dimensions in this diagram are all in mm.

screens were fastened on top of these tubes to allow the entry of rain and snow but not large organic materials (e.g., falling leaves in autumn).

2.2.2. Initial conditions, sensor locations and effluent collection

The physical properties of the columns and details of the initial conditions of the experiment are summarized in Table 1. Four columns were constructed to elucidate the effects of three parameters: water saturation/content, particle size distribution and column thickness. In case 1 or reference column, the thickness was 600 mm with a particle size distribution of <2 mm in diameter. The lithology of the crushed rock in this column is classified as loamy sand composed of 89.4% sand, 5.3% fine sand and 5.3% silt. The bottom of the reference column was open to the atmosphere so water flow was gravity-controlled. With this configuration, a distinct vertical distribution of the water content is developed close to steady state conditions, that is, the bottom part is almost saturated but the middle and upper regions remained largely unsaturated (Tabelin et al., 2012c). To avoid confusion, we will refer to this condition as "free-flow" throughout this paper. The second column (case 2) was constructed identical to the first one, but placed in the PVC tube with a bottom adjustable valve and a manometer-like transparent tube to control the flow of water and observe the water level, respectively (Fig. 1). The bottom valve was opened once the column is fully saturated and then closed after all the water had been drained. This condition wherein the column was first allowed to fully saturate prior to

Table 1
List of column experimental conditions.

Case	Column name	Particle size distribution	Thickness of column (mm)	Mass of rock (kg)	Bulk density (g/cm^3)	Sensor location from the surface of the column (mm)	
						PO_2	Temperature + θ + EC
1	Free-flow	<2 mm	600	66	1.58	435	435
2	Controlled-flow	<2 mm	600	66	1.58	440	440
3	Gravel	2–9.5 mm	600	66	1.58	418	418
4	Thickness = 300 mm	<2 mm	300	33	1.58	none	none

Note: Free-flow, Loamy sand and Thickness = 600 mm are the same columns.

the collection of effluent samples would be referred to as "controlled-flow" throughout this paper. To elucidate the effects of particle size distribution, a third column (case 3) was constructed with the same amount of rock as case 1 but with 100% gravel-sized particles (2–9.5 mm). This narrow range of particle size was achieved by sieving. Finally, the fourth column (case 4) had the same bulk density and particle size distribution as case 1, but only half in thickness (300 mm) to evaluate the effect of column thickness on the migration of trace elements. All columns were initially dry and irrigation was only supplied by rain and melting snow.

Two kinds of sensors were set inside the columns as shown in Fig. 1: (1) 5TE (Decagon Devices, Germany) measured the temperature, volumetric water content (θ), and electrical conductivity (EC) simultaneously, and (2) MIJ-03 (Environmental Measurement Japan Co., Ltd., Japan) tracked the real time changes in partial pressure of oxygen (PO_2). These sensors were placed during the packing of crushed sample in three of the columns (cases 1, 2 and 3) with their respective locations listed in Table 1. Measurements of temperature, θ, EC and PO_2 within the columns commenced on May 18, 2009 (4 pm) and ended on August 17, 2011 (11 am). The time interval of each measurement was 1 h, and the data were stored in data loggers installed on site (Em50, Decagon Devices, Germany). The volume of effluent generated by the columns was constantly monitored and once the sampling bottles were almost full, they were collected and replaced. This means that effluent collection was more frequent during the spring–summer–autumn months when rainfall was substantial. The pH, redox potential (Eh) and EC of the effluents were measured immediately after sample collection. This was followed by filtration of the effluents through 0.45 μm Millex® membrane filters (Merck Millipore, USA), and the filtrates were then divided into three parts for the analyses of alkalinity, trace elements and coexisting ions. The portion for the measurements of trace element concentrations was preserved by acidification (pH < 2) and cold storage (6 °C).

2.3. Chemical analyses

Concentrations of As, Se and B were measured using an inductively coupled plasma mass spectrometer (ICP-MS) (Agilent 7500cx, Agilent Technologies Inc., USA) while that of iron (Fe) was quantified using an inductively coupled plasma atomic emission spectrometer (ICP-AES) (Optima 4300DV, PerkinElmer Inc., USA). Dissolved silica (Si) and calcium (Ca) were determined using the molybdenum blue calorimetric method and atomic absorption spectrometry (AAS) (Aanalyst 200, PerkinElmer Inc., USA), respectively. Concentrations of major cations (Na^+, K^+ and Mg^{2+}) and anions (Cl^- and SO_4^{2-}) were measured using cation (ICS-90, Dionex Corporation, USA) and anion chromatographs (ICS-2000, Dionex Corporation, USA), respectively. Bicarbonate (HCO_3^-) and carbonate (CO_3^{2-}) ion concentrations were estimated from the pH and alkalinity using PHREEQC (Parkhurst and Appelo, 1999). The latter was measured by titration of a known volume of filtered effluent with 0.02 N sulfuric acid (H_2SO_4) solution until pH 4.8. Measurements using the ICP-AES, AAS and ion chromatographs have margins of error between 2 and 3% while those of the ICP-MS had uncertainties of ca. 5%.

2.4. Calculation of leachability, geochemical modeling and mass balances

Leachability, L_i (mg/kg or μg/kg), of a particular element was calculated from the measured concentrations, C_i (mg/L or μg/L), and normalized to the mass of the tunnel-excavated rock, where i denotes the element:

$$L_i = \frac{C_i * V_L}{m_r}.$$

V_L (L) is the volume of effluent collected in each sampling campaign and m_r (kg) is the mass of tunnel-excavated rock in the column. Leachability is better than concentration in the comparison of results because the volume of effluents collected and mass of rock used differed between the columns.

Saturation indices (*SIs*) of minerals that could influence the mobilities of As, Se and B, like Fe-oxyhydroxide and clay minerals, were calculated using PHREEQC. For these calculations, the THERMODDEM database, compiled by the French Geological Survey (BGRM Institute), was used (Blanc et al., 2012). Additional minerals of As ($Ca_3(AsO_4)_2 \cdot 3H_2O$, $CaHAsO_4 \cdot 4H_2O$, $MgHAsO_4$ and $Mg(AsO_4)_2$), Se ($CaSeO_3$, $CaSeO_3 \cdot 2H_2O$, $MgSeO_3$ and $MgSeO_3 \cdot 6H_2O$) and B (colemanite ($CaB_3O_4(OH)_3 \cdot H_2O$) and pinnoite ($MgB_2O(OH)_6$)) were included in the calculations because of the significant concentrations of Ca^{2+} and Mg^{2+} in the effluents (Supplementary Table 1). The speciation of As, Se and B under in situ conditions was evaluated using Eh–pH stability diagrams created with the Geochemist's Workbench® based on the actual solute activities of these trace elements in the effluents (Bethke, 1992).

3. Results

3.1. Effects of free- and controlled-flow conditions on the effluent chemistry and the leaching of arsenic, selenium and boron

The average flow rate of the free-flow column (0.158 cm/day) was relatively faster than that of the controlled-flow column (0.101 cm/day) because the latter was allowed to fully saturate prior to effluent collection. In terms of the temperature, θ and EC within the columns, all of them fluctuated cyclically with the four seasons of Hokkaido independent of the flow condition (Supplementary Fig. 4). In the first 4 months of monitoring, the θ and EC readings strongly fluctuated depending on the degree/intensity of rainfall since both columns were initially dry. In addition, PO_2 level in the controlled-flow column decreased rapidly after reaching full saturation while that in the free-flow column was virtually constant. After this period, the effects of rainfall on these three parameters became negligible indicating that apparent steady state conditions had been reached. This condition was, however, interrupted at the start of winter due to the drop in temperature that limited irrigation and caused the porewater to freeze. This freezing episode persisted for ca. 4 months and within this period, the θ and EC values were very low in both the free- and controlled-flow columns. After the temperature rose above 0 °C by the end of winter, the melting of pore water and thawing of snow both contributed to the rapid return of the θ and EC back to their pre-winter levels. The strong effects

of freezing and thawing episodes on these parameters were again observed in the succeeding year of the experiment.

The pH measured from the first effluents of the two columns were similar (ca. pH 8) and both of them rapidly increased in the next effluents (Fig. 2(a)). Although the initial pH trends were similar in the two cases, the free-flow column appears to have higher pH values than the controlled-flow column in the first 6 months of the experiment. After this, however, the pH values in the free-flow column decreased and remained lower than those of the controlled-flow column. Regardless of these differences, effluent pH values of the two columns approached a similar range of values towards the end of the experiment (pH: 8–9.2), indicating that both cases reached apparent equilibrium.

The leaching of As under free-flow condition was initially very high, but rapidly decreased as more rainwater passed through the column (Fig. 2(b)). In comparison, the leaching of As in the controlled-flow column significantly decreased (40–60%) during the first two sampling campaigns. The leachability curve in this column also had a distinct initial peak that was absent in the free-flow column. Moreover, the decrease in As leachability was more gradual in the controlled-flow column than that in the free-flow column. Regardless of these differences, leaching concentrations of As from May-2009 to January-2010 in both cases exceeded the Japanese environmental standards (10 μg/L) (Supplementary Fig. 6). During the second year of the experiment, the leaching trends of As continued to differ depending on the flow condition. The leachability of As in the controlled-flow column was lower and nearly constant while that under free-flow condition varied with the seasons similar to the θ (Supplementary Fig. 4(b)). This strong influence of water flow and degree of saturation on the release of As was also supported by the leached mass percentage calculations. The total amount of As leached from the free-flow column was almost twice as high as that of the controlled-flow column (Table 2).

The leaching curves of Se under free- and controlled-flow conditions followed similar tendencies, that is, both had initial flushing-out trends subsequently followed by wave-like patterns (Fig. 2(c)). In the controlled-flow column, however, Se leachability was apparently lower than that in the free-flow column after May-2010. This observation is corroborated by the leached mass percentage calculations, which showed that the total amount of Se released from the former decreased by ca. 17% (Table 2). Although Se leachability decreased under this condition, the leaching concentration of Se in the effluent still exceeded the Japanese environmental standard until the end of the experiment (Supplementary Fig. 6).

During the first 6 months, the leaching of B in the free-flow column fluctuated cyclically with the frequency and intensity of rainfall while that under controlled-flow condition was nearly constant (Fig. 2(d); Supplementary Fig. 2). In the succeeding months, however, the leaching curve of B in the controlled-flow column closely followed the wave-like pattern exhibited by B in the free-flow column. It is also interesting to note that the leachability of B in the controlled-flow column

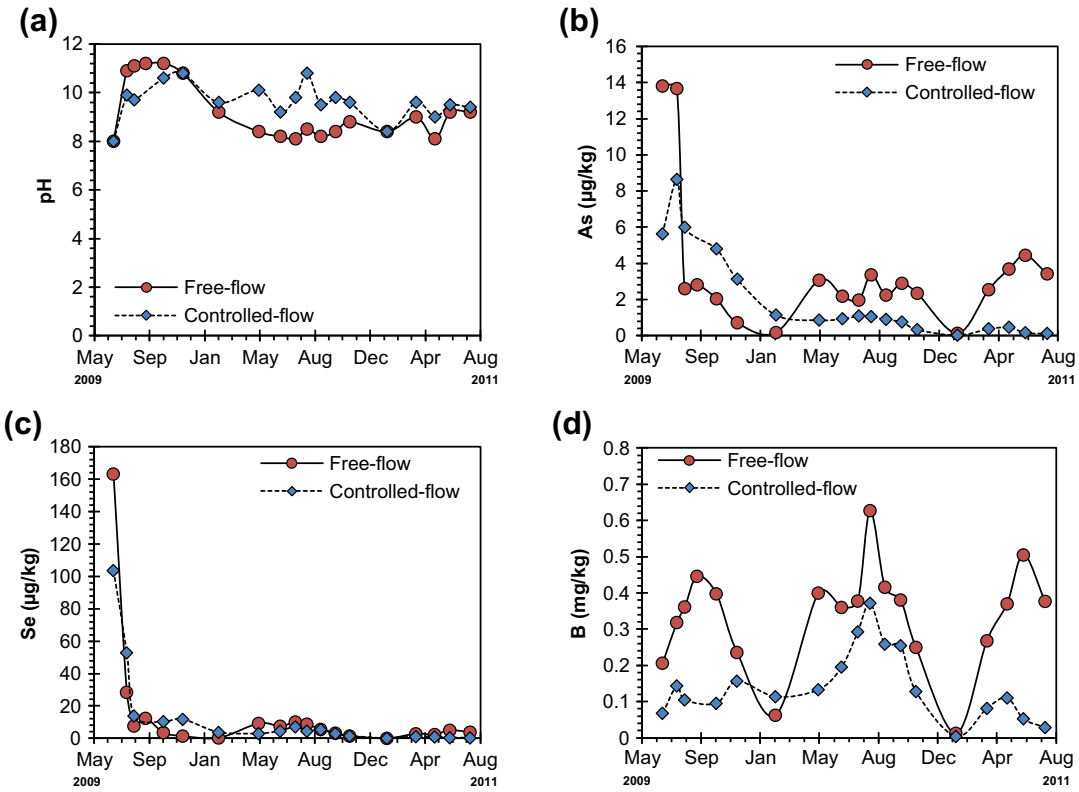

Fig. 2. Evolution of effluent pH and the leachabilities of As, Se and B under free- and controlled-flow conditions; (a) effluent pH change with time, (b) change of As leachability with time, (c) change of Se leachability with time, and (d) change of B leachability with time.

Table 2
Total masses of As, Se and B leached during the in situ column experiments.

Case	Condition	Mass leached (mg)			Mass leached (% of total)		
		As	Se	B	As	Se	B
1	Free-flow	4.49	18.3	421	0.76	47	5.6
2	Controlled-flow	2.4	15.1	171	0.4	39	2.3
3	Gravel	4.48	17.9	449	0.75	46	6
4	Thickness = 300 mm	3.12	9.6	335	1.05	49	9

was consistently lower than that under free-flow condition. Overall, the total amount of B leached from the free-flow column was ca. 2.5-times higher than that of the controlled-flow column (Table 2). Similar to As and Se, the leaching concentrations of B in both cases exceeded the Japanese environmental standard throughout the duration of the experiment (Supplementary Fig. 6).

3.2. Effects of particle size distribution on the effluent chemistry and the leaching of arsenic, selenium and boron

Temperatures measured within the columns with loamy sand- and gravel-sized aggregates were nearly identical, but their θ, PO_2 and EC values substantially differed (Supplementary Fig. 5). The θ values recorded in the column with finer-sized aggregates were higher (0.1–0.5) than those of the column with larger-sized particles (0.04–0.2), indicating that the former retained more water than the latter (Supplementary Fig. 3). In winter and early spring, the rapid decrease and increase of the θ due to freezing and thawing, respectively, were also less apparent in the column with gravel-sized aggregates. This difference could be attributed to lower θ values in the column with larger aggregates. According to Van Bochove et al. (2000), the effect of freezing in soils was stronger in those with finer aggregates largely because of their higher water content. Initial PO_2 values of the gravel- and loamy sand-sized columns were identical and both decreased gradually as irrigation commenced from rainfall in spring. The decline in PO_2 was, however, conspicuously faster in the finer-sized column and by mid-summer, the PO_2 level dropped to ca. 1.5% below that of the gravel-sized column. As mentioned previously, the decrease in PO_2 became more extensive under saturated condition. Because the gravel-sized column did not reach saturated conditions even near the bottom of the rock bed, the PO_2 level was higher and nearly constant. Similar to θ, EC values of the column with larger-sized aggregates were generally lower than those with finer-sized aggregates.

Fig. 3 shows the evolution of effluent pH and the leachabilities of As, Se and B in the columns with loamy sand- and gravel-sized aggregates. During the first 9 months of the study, both of the columns exhibited "hill"-shaped patterns in their pH curves (Fig. 3(a)). However, the pH of the gravel-sized column plateaued at a slightly lower level. The following year, the pH curve of this column again exhibited the same "hill"-like

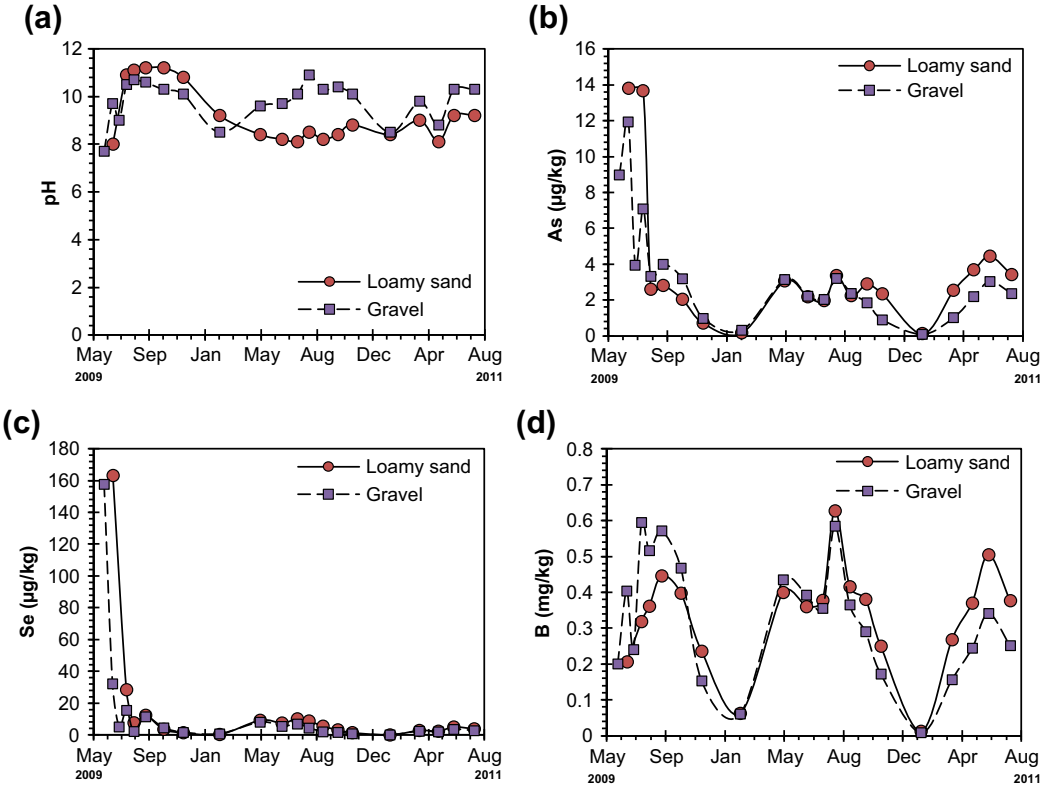

Fig. 3. Evolution of effluent pH and the leachabilities of As, Se and B in the columns with loamy sand- and gravel-sized aggregates; (a) effluent pH change with time, (b) change of As leachability with time, (c) change of Se leachability with time, and (d) change of B leachability with time.

pattern, but was missing in the column with finer aggregates. Rather than increase and decrease with the seasons, the effluent pH of the loamy sand-sized column was nearly constant during this period. Additionally, the pH values measured in this column during the latter period of the experiment were consistently lower than those of the column with larger aggregates.

The leachabilities of As and Se in the two columns of different particle size distributions followed identical trends (i.e., initial flushing-out followed by a somewhat wave-like pattern) (Fig. 3(b) and (c)). Regardless of such similarities, it is important to note that the leachabilities of both As and Se slightly decreased initially in the column with larger aggregates. This reduction was so small, however, that the total amounts of As and Se leached from the two cases were nearly the same (Table 2). The effect of particle size distribution was slightly more apparent in the leachability of B as illustrated in Fig. 3(d). There are three clear patterns illustrated in this figure: (1) higher B leaching in the column with larger aggregates during the first 6 months, (2) nearly identical B leaching in the two columns in the succeeding 15 months, and (3) lower B leaching in the column with larger aggregates in the final 6 months of the experiments. This general trend of more rapid decrease in B leachability is supported by the leached mass percentage calculations (Table 2), indicating that B was more rapidly mobilized in the column with larger aggregates. Even though the leachabilities of As, Se and B decreased year after year, the effluents collected from the column with gravel-sized aggregates still had concentrations of trace elements that exceeded the Japanese environmental standards (Supplementary Fig. 7).

3.3. Effects of column thickness on the effluent chemistry and the leaching of arsenic, selenium and boron

The pH of the first effluent collected from the 300 mm-thick column was ca. 2 pH units higher than that of the 600 mm-thick column (Fig. 4(a)). However, the succeeding effluents from this column had pH values nearly identical with those of the thicker column. In addition, both columns exhibited initial plateaus in their pH curves that disappeared the following year. The leaching concentrations of As and B were relatively lower in the thinner column (Supplementary Fig. 8). These results are to be expected because the 600 mm-thick column contained twice as much rock as the 300 mm-thick column. When these values are normalized to the mass of the rock, it is easier to recognize that the total amounts of As and B leached were actually higher in the thinner column by ca. 28 and 37%, respectively (Table 2). This is also clearly illustrated in the leachability curves of As and B illustrated in Fig. 4(b) and (d). In comparison, the leachability of Se was slightly reduced in the 300 mm-thick column but only during the first 3 months of the experiment. After this, the leaching curves of Se in the two columns were virtually identical. The period of time in which the leachability of Se decreased was fairly short in comparison with those of As and B. Furthermore, the total amounts of Se released from the two columns were nearly equal after normalization (Table 2).

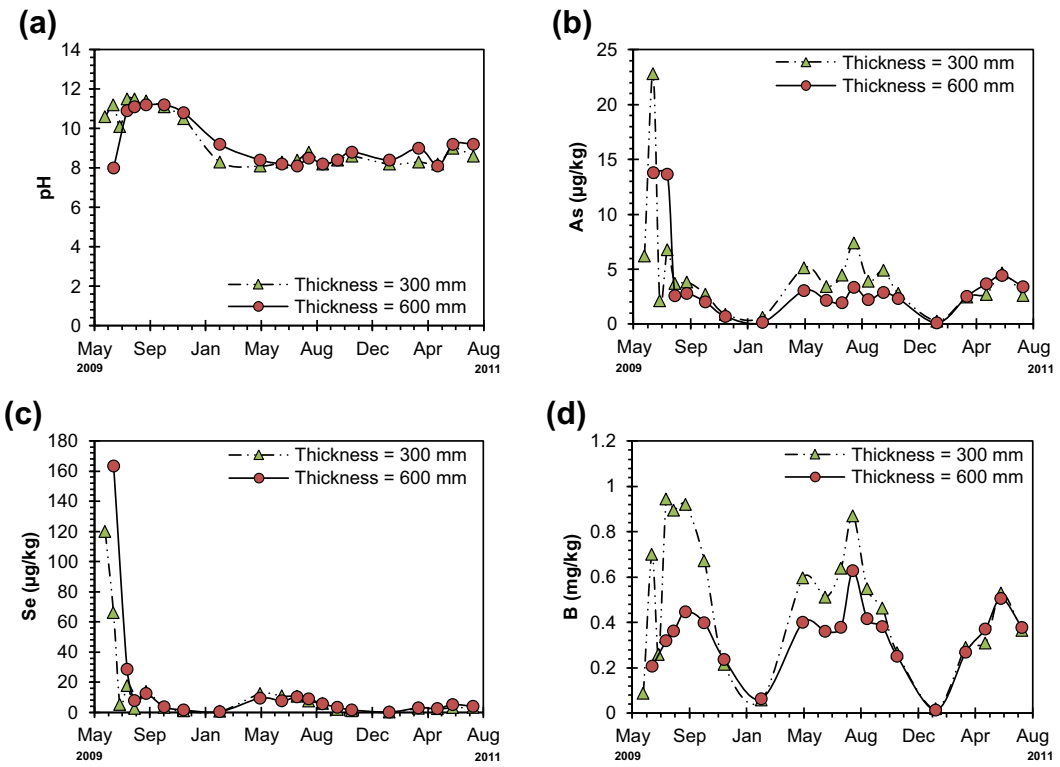

Fig. 4. Evolution of effluent pH and the leachabilities of As, Se and B in the 300 and 600 mm-thick columns; (a) effluent pH change with time, (b) change of As leachability with time, (c) change of Se leachability with time, and (d) change of B leachability with time.

These results indicate that in the long term, Se leaching is fairly unaffected by changes in the column thickness.

3.4. Piper diagram and the leachability of coexisting ions

Fig. 5 is a piper diagram showing the type of effluents produced by the sedimentary rock sample under the various conditions evaluated in this study. Except for a single sample, the rest exhibited Na^+–SO_4^{2-} type hydrochemical facies, indicating that changes in the type of flow/water content, thickness and particle size distribution did not affect the type of leachate generated by the rock. These results also indicate that Na^+ is the major cation and SO_4^{2-} is the dominant anion under in situ conditions. Little change in the relative distributions of these major ions suggests that seasonal variations in precipitation as well as the freezing–thawing events in winter do not dramatically alter the major ion chemistry of the effluents. Comparing these results with our previous work (Tabelin et al., 2014b) would also show that the type of effluent produced by sedimentary rocks upon exposure to the environment could be reliably predicted by simply adjusting the liquid-to-solid ratio used in laboratory reactor-type experiments.

Although a piper diagram could easily identify the major ions in the effluent, it does not clearly illustrate how these ions varied with time. Moreover, it is difficult to compare the evolution of the major ions with those of the toxic elements using this diagram alone. Thus, the leachabilities of the coexisting ions like Ca^{2+}, Na^+, SO_4^{2-}, HCO_3^-, CO_3^{2-} and Cl^- are presented as supplementary data (Supplementary Figs. 9–11). The leaching curves of most of the major coexisting ions (i.e., Ca^{2+}, Na^+, SO_4^{2-} and Cl^-) in the free-flow column had flushing-out trends similar to those of the EC (Supplementary Fig. 9). Only the leachability curve of $HCO_3^- + CO_3^{2-}$ was distinctly different, which had a slight peak in place of the initial rapid decrease characteristic of flushing-out trends (Supplementary Fig. 9(e)). Although the effect of controlled-flow (i.e., more saturated conditions) on the evolution of the effluent EC was a bit ambiguous (Supplementary Fig. 9(a)), its importance became obvious in the leachability curves of the major coexisting ions. First, allowing the column to become more saturated minimized the initial leaching of most of the major ions (e.g., Ca^{2+}, Na^+, SO_4^{2-} and Cl^-) and second, this condition delayed the release of the more reactive HCO_3^- or CO_3^{2-} ions. The same leachability trends were also observed in the columns with different particle size distributions and thicknesses, indicating that $HCO_3^- + CO_3^{2-}$ was much more reactive compared with the other dissolved ions.

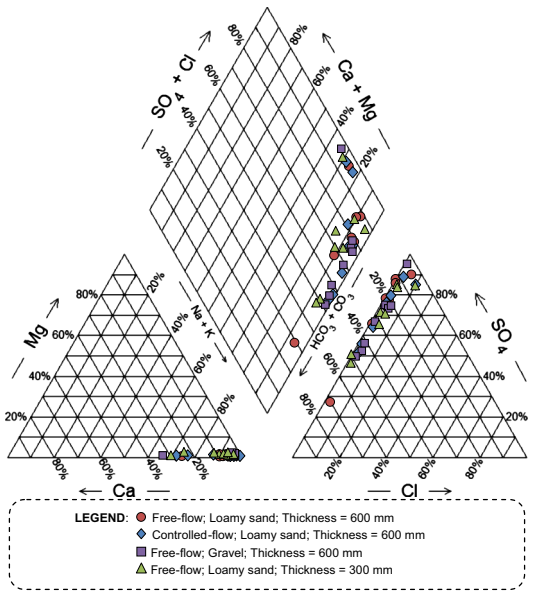

Fig. 5. Piper diagram showing the hydrochemical facies of effluents collected under in situ conditions.

4. Discussion

There are several geochemical processes controlling the release of As, Se and B from sedimentary rocks under in situ conditions. These processes are all interrelated, but the magnitude of their effects on the overall leaching of the trace elements changed with time. In the case of As and Se, two distinct regions were present in their leaching curves, suggesting two different sets of processes controlling their release in sedimentary rock–water systems. The first region lasted only for 6 months, indicating that the processes controlling the leachabilities of As and Se in this region could be considered as the short-term mechanisms of release. This period was characterized by flushing-out trends, indicating that these two elements were rapidly released and transported out of the columns. The rapid release of As and Se most likely occurred due to the dissolution of soluble phases like evaporite salts, which contain significant amounts of these elements. This interpretation is supported by the consistently strong and statistically significant positive correlations of As and Se with ions that generally constitute evaporite salts like Na^+, Ca^{2+} and SO_4^{2-} independent of the column conditions (Supplementary Tables 2–5). In addition, these results validated our previously proposed model that highlighted the important role of soluble salts in the leaching of As and Se from marine sedimentary rocks (Tabelin et al., 2014c).

The leaching curves of As and Se also showed that the release of the former was somehow minimized initially but not that of latter, indicating that immobilization reactions may affect the mobility of As more than that of Se. Although relatively high concentrations of Ca^{2+} were measured during the first 6 months of the study, precipitation of As and Se as Ca-arsenate and Ca-selenites, respectively, were thermodynamically unfavorable (Supplementary Fig. 12). This leaves adsorption as the only probable immobilization mechanism of these two trace elements. The rock sample used in this study contains minor amounts of smectite and based on our geochemical modeling calculations, precipitations of Fe-oxyhydroxides and calcite during the experiments were thermodynamically favorable (Supplementary Fig. 13). Fe-oxyhydroxides and clay minerals are well known for their As and Se adsorption capabilities (Bar-Yosef and Meek, 1987; Cornelis et al., 2008; Dzombak and Morel, 1990; Fendorf et al., 1997; Lin and Puls, 2000; Manning et al., 1998; Peak and Sparks, 2002) while calcite had been recently shown to incorporate Se in its crystal structure (Renard et al., 2013), indicating that these minerals

may be responsible for the observed As and Se immobilization. Although both As and Se are adsorbed onto Fe-oxyhydroxide and clay minerals, As adsorption was greater because of two reasons: (1) As adsorption was moderately enhanced in the presence of high concentrations of Ca^{2+} (Meng et al., 2000; Wilkie and Hering, 1996), and (2) the bulk of As existed as arsenate (As[V]) while that of Se was as selenate (Se[VI]) (Supplementary Figs. 14 and 15). These two species have very contrasting adsorption properties. Whereas As[V] binds strongly onto both Fe-oxyhydroxides and clay minerals through the formation of inner or outer sphere complexes (Fendorf et al., 1997; Manning et al., 1998), Se[VI] is rarely adsorbed onto such minerals (Balistrieri and Chao, 1987; Kang et al., 2002). In addition, calcite only incorporates selenite (Se[IV]) in its crystal structure and not Se[VI] (Renard et al., 2013). These mean that although As and Se were simultaneously released via the dissolution of soluble salts, the former was less mobile than the latter due to its stronger adsorption onto minerals like Fe-oxyhydroxides and clays.

The second region of the leaching curves of As and Se was characterized by a distinct wave-like pattern with the wave's crest and trough positioned around summer and winter, respectively (Figs. 2, 3 and 4). This region lasted for almost 2 years and would most likely continue for a long time, so the dominant processes controlling the leaching of As and Se during this period could be considered as their long-term release mechanisms. This wave-like pattern was not unique to the leaching curves of As and Se, but was also prominent in those of Ca^{2+} and SO_4^{2-}. Because most of the soluble salts had been dissolved and flushed-out of the column in this latter period, the remaining sources of Ca^{2+} and SO_4^{2-} in the rock are calcite/plagioclase and pyrite, respectively. Plagioclase is a solid-solution of albite (Na–Al silicate mineral) and anorthite (Ca–Al silicate mineral), so the bulk of Ca^{2+} contributed by the dissolution of plagioclase originated from the latter. Although anorthite is less soluble than calcite, it is important to note that both are important sources of Ca^{2+} under in situ conditions. Oxidation of pyrite produces acidity that is used up in the dissolution of calcite and anorthite according to the following reactions:

$$FeS_{2(s)} + \frac{15}{4}O_2 + \frac{5}{2}H_2O \rightarrow FeOOH_{(s)} + 4H^+ + 2SO_4^{2-} \quad (1)$$

$$2FeS_{2(s)} + \frac{15}{2}O_2 + 4H_2O \rightarrow Fe_2O_{3(s)} + 8H^+ + 4SO_4^{2-} \quad (2)$$

$$FeS_{2(s)} + \frac{15}{4}O_2 + \frac{7}{2}H_2O \rightarrow Fe(OH)_{3(s)} + 4H^+ + 2SO_4^{2-} \quad (3)$$

$$CaCO_{3(s)} + H^+ \rightarrow Ca^{2+} + HCO_3^- \quad (4)$$

$$CaAl_2Si_2O_{8(s)} + 8H^+ \rightarrow Ca^{2+} + 4H_2O + 2Al^{3+} + 2SiO_{2(aq)}. \quad (5)$$

The crest of the wave-like leaching curves of As, Se, Ca^{2+} and SO_4^{2-} coincided well with the summer months of the year when rainfall was abundant. This means that the release of As and Se was enhanced during this period because of two reasons: (1) PO_2 in the pore water was rapidly replenished and promoted the oxidation of pyrite (Supplementary Fig. 4(c); Eqs. (1)–(3)), which contains substantial amounts of these elements, and (2) adsorption of As and Se was minimized by the rapid water infiltration. Adsorption/desorption of As and Se became more significant in the long term because of the low solute activities of both elements. On the other hand, the trough of the wave-like leaching curves happened in winter when the bulk of pore water froze. This freezing episode curtailed both the oxidation of pyrite and adsorption by limiting the amount of available O_2 and the functional liquid pore water within the columns. These interpretations are consistent with the θ and PO_2 curves as well as the very low leaching of SO_4^{2-} and Ca^{2+} during this period (Supplementary Figs. 4 and 9).

The solid-phase partitioning of B closely resembled that of As and Se, that is, considerable amounts of B were also partitioned with the soluble phases (Tabelin et al., 2014b). However, its leaching curve did not have the flushing-out trend observed in those of As and Se. In its place was the same distinct wave-like pattern only exhibited by the leaching curves of As and Se in the latter part of the study. Initially, these three trace elements were simultaneously released due to the dissolution of soluble salts as explained earlier. Moreover, all three trace elements are known to adsorb onto Fe-oxyhydroxides and clay minerals, which are present in the sedimentary rock sample. Therefore, the disappearance of the flushing-out trend in the case of B indicates that this element was more strongly adsorbed than As and Se during this period. Because both B and As are strongly adsorbed onto Fe-oxyhydroxides between pH 7 and 10 (Dzombak and Morel, 1990; Goldberg and Glaubig, 1985), the large discrepancy in their leaching behaviors could be explained by their pH-dependent adsorption maxima onto clay minerals. According to Frost and Griffin (1977), As[V] adsorption onto clay minerals like kaolinite and montmorillonite peaked between pH 4 and 6, substantially decreasing at higher pH values. In contrast, the adsorption maxima of B in these two clay minerals occurred in the pH range of 8–10 (Goldberg et al., 1996). Effluent pH values measured during the first 6 months of the study was between 8 and 11 that coincided well with the adsorption maxima of B onto clay minerals. In addition, the release of B during this period was retarded more strongly than As because of the high concentrations of Ca^{2+} and Na^+ that promoted its adsorption onto clay minerals (Goldberg et al., 1993; Keren and O'Connor, 1982; Keren and Sparks, 1994; Mattigod et al., 1985). In the presence of high concentrations of Ca^{2+} and Na^+, B is more readily adsorbed because these positively-charged ions suppress the negative electrical field surrounding the planar surface of clay minerals (Keren and O'Connor, 1982; Keren and Sparks, 1994). Although relatively rapid and extensive, the adsorption of B was only temporary due to its weak bonding onto clay particles via outer sphere complexation (Majidi et al., 2010). As a result, adsorbed B was gradually re-mobilized with time as the concentrations of the cations decreased. By comparing the leaching curves and leached mass percentages of B and As, this re-mobilization of B following its rapid adsorption was also apparent in this study (Fig. 2; Table 2). From the leaching curves, adsorption of B was more extensive than that of As during the first part of the study. Later on, however, both of these elements were released via similar

mechanisms (i.e., pyrite oxidation and adsorption/desorption). If we assume that both B and As are not re-mobilized, the mass balance results should show that the total amount of As leached out of the rock is relatively higher than that of B because adsorption of the latter is clearly greater than that of the former. However, our calculations showed that the total mass of As released from the rock (i.e., normalized to the total content of the rock) was consistently lower than that of B in all of the columns (Table 2). This means that although B was rapidly adsorbed, it was gradually re-mobilized in the latter part of the experiment. Finally, the pH-driven de-protonation of boric acid from $B(OH)_3$ to $B(OH)_4^-$ probably occurred in the study, but this had insignificant effects on the adsorption of B especially in the early stages of the experiment (Supplementary Fig. 16).

Under in situ conditions, the extent of processes like dissolution, adsorption/desorption and pyrite oxidation is closely related to θ and water residence time. This is because θ controls the effective reaction area within the column while water residence time is closely related to the reaction time. However, both θ and water residence time are dependent variables, which are also influenced by environmental factors (e.g., frequency/intensity of rainfall) as well as the physical properties of the rock (e.g., particle size distribution). This means that environmental factors and the physical properties of the rock both play important but indirect roles in the leaching of trace elements in sedimentary rock–water systems. In this study, both precipitation and temperature were crucial in water infiltration and percolation because the experiment was conducted under a humid continental climate (i.e., warm to hot summer and cold to severely cold winter). From spring to autumn, water infiltration and percolation were controlled by the rainfall frequency/intensity because precipitation as rain was quite abundant. In winter, however, both water infiltration and percolation were restricted by the temperature rather than the intensity/frequency of precipitation. The bulk of precipitation during this period was comprised of "fluffy" snow, which did not melt even after falling on the surface of the columns because of the sub-zero temperatures. As a result, water infiltration was effectively minimized and precipitation throughout winter just accumulated on top of the columns. Another consequence of the sub-zero temperatures was the freezing of pore water within the columns that limited percolation. By the end of winter, the temperature again played a critical role in water infiltration and percolation. As soon as it rose a little bit above zero, the frozen pore water and snow cover rapidly thawed and melted, respectively, which quickly brought the θ back to its pre-winter levels. This freezing–thawing events as well as the limited infiltration during this season were strongly implied by the distinct patterns of θ as well as the volume of effluents collected in the columns (Supplementary Figs. 3–5). Limited infiltration in conjunction with the freezing of pore water during winter minimized the leaching of trace elements due to the decreased effective reaction area. However, the rapid thawing in spring as well as the abundant rainfall in summer enhanced the mobility of trace elements because water infiltration and percolation were faster and easier (i.e., shorter water residence time). The strong influence of water residence time and θ was also observed by increasing the degree of saturation prior to sample collection (i.e., controlled-flow column). Our calculations showed that the total amounts of As, Se and B leached from the rock decreased by ca. 18, 10 and 65% under such conditions, indicating that higher degree of saturation and longer water residence time minimized the leachabilities of these trace elements most likely due to enhanced adsorption (Table 2). In contrast, reducing the thickness of the column resulted in shorter water residence time that increased the leaching of these trace elements (Table 2).

Initial conditions of the column experiments also affected both θ and water residence time. For example, the total pore volume (i.e., open space inside the column accessible to water) as well as the morphology of pores within the column depend on the particle size distribution. The column with gravel-sized aggregates had a much lower total pore volume compared with the loamy sand-sized aggregates, but the pores of the former were relatively bigger and more interconnected than the latter. These large and well-defined pores allowed water to pass through more easily, which resulted in shorter water residence time. The size distribution of particles also directly affected the amount of water retained within the columns (Supplementary Fig. 3). Bigger pores of the gravel-sized column held on to less water than the finer-sized column especially under the conditions of this study. This kind of setup also promoted depth-dependent distribution of pore water within the column as reported in our previous work (Tabelin et al., 2012c). Such non-uniform water distribution, however, became less prominent as the particle size increased as implied by the consistently unsaturated conditions of the column with larger aggregates (Supplementary Fig. 3). The size of aggregates also strongly influenced the leachability of B but not those of As and Se most likely because B is more readily adsorbed onto fine-sized particles (Majidi et al., 2010). From our rough estimates using the results of this study and the assumption that only trace elements partitioned with exchangeable and sulfide phases would be released, concentrations of As, Se and B in the effluent will most probably continue to exceed the environmental standards for at least 306, 2.2 and 5.2 more years, respectively, even if a variety of conditions are considered.

5. Conclusion

The results of this study have several important implications in the management of sedimentary rocks containing hazardous trace elements like As, Se and B excavated from tunnel projects. First, although sedimentary rocks may only contain background levels of hazardous trace elements, they could produce leachates with concentrations of these elements exceeding the environmental standards when exposed to the environment. Second, these trace elements behave differently under in situ conditions, so a single countermeasure might not be appropriate to address the problem posed by all three elements. For example, the use of Fe- or Al-based adsorbents might reduce the leaching of As but not those of Se and B. Because of this, a combination of several countermeasures, each targeting one of the trace contaminants, might be more appropriate. Third, the leaching of these trace elements is hardly influenced by the particle size distribution of the rock, so crushing as well as size classification techniques would not be applicable.

Acknowledgment

The authors wish to thank Hokkaido Regional Development Bureau of the Ministry of Land, Transport and Tourism for providing us with the sample and test area for the in situ experiments as well as the anonymous reviewers for their valuable inputs to this paper. Part of this research was supported by the Japan Society for the Promotion of Science (JSPS) grant-in-aid for scientific research (grant number: 26289149).

Appendix A. Supplementary data

Supplementary data to this article can be found online at http://dx.doi.org/10.1016/j.jconhyd.2015.01.003.

References

Ayaz, M., Dalkilic, N., Tuncer, S., Bariskaner, H., 2008. Selenium-induced changes on rat sciatic nerve fibers: compound action potentials. Methods Find. Exp. Clin. Pharmacol. 30, 271–275.

Balistrieri, L.S., Chao, T.T., 1987. Selenium adsorption by goethite. Soil Sci. Soc. Am. J. 51, 1145–1151.

Bar-Yosef, B., Meek, D., 1987. Selenium sorption by kaolinite and montmorillonite. Soil Sci. 144 (1), 11–19.

Bethke, C.M., 1992. The Geochemist's Workbench — a User's Guide to Rxn, Act2, Tact, React and Gtplot. University of Illinois-Urbana, Illinois.

Beyer, K.H., Bergfield, W.F., Berndt, W.O., Boutwell, R.K., Carlton, W.W., Hoffman, D.K., Schroeter, A.L., 1983. Final report on the safety assessment of sodium borate and boric acid. J. Am. Coll. Toxicol. 2, 87–125.

Bjørlykke, K., 2013. Relationships between depositional environments, burial history and rock properties: some principal aspects of diagenetic process in sedimentary basins. Sediment. Geol. 301, 1–14.

Blanc, Ph., Lassin, A., Piantone, P., Azaroual, M., Jacquemet, N., Fabbri, A., Gaucher, E.C., 2012. Thermoddem: a geochemical database focused on low temperature water/rock interactions and waste materials. Appl. Geochem. 27, 2107–2116.

Brtko, J., Filipcik, P., 1994. Effect of selenite and selenate on rat liver nuclear 3,5,3′-triiodothyronine (T3) receptor. Biol. Trace Elem. Res. 41, 191–199.

Cebrian, M.E., Albores, A., Aquilar, M., Blakely, E., 1983. Chronic arsenic poisoning in the North of Mexico. Hum. Toxicol. 2, 121–133.

Chakraborty, A.K., Saha, K.C., 1987. Arsenical dermatosis from tubewell water in West Bengal. Indian J. Med. Res. 85, 326–334.

Chatterjee, M., Banerjee, M.R., 1982. Selenium mediated dose-inhibition of 7,12-dimethylbenz[a] anthracene-induced transformation of mammary cells in organ culture. Cancer Lett. 17, 187–195.

Chen, C.J., Chuang, Y.C., Lin, T.M., Wu, H.Y., 1985. Malignant neoplasms among residents of a blackfoot disease-endemic area in Taiwan: high-arsenic artesian well water and cancers. Cancer Res. 45 (11), 5895–5899.

Chen, C.J., Chen, C.W., Wu, M.M., Kuo, T.L., 1992. Cancer potential in liver, lung, bladder and kidney due to ingested inorganic arsenic in drinking water. Br. J. Cancer 66 (5), 888–892.

Cornelis, G., Anette-Johnson, C., Van Gerven, T., Vandecasteele, C., 2008. Leaching mechanisms of oxyanionic metalloid and metal species in alkaline solid wastes: a review. Appl. Geochem. 23, 955–976.

Dzombak, D.A., Morel, F.M.M., 1990. Surface Complexation Modeling: Hydrous Ferric Oxide. John Wiley and Sons, New York.

Fendorf, S., Eick, M.J., Grossel, P., Sparks, D.L., 1997. Arsenate and chromate retention mechanisms on goethite. 1. Surface structure. Environ. Sci. Technol. 31, 315–320.

Fishbein, L., 1983. Environmental selenium and its significance. Fundam. Appl. Toxicol. 3, 411–419.

Frost, R.R., Griffin, R.A., 1977. Effect of pH on adsorption of arsenic and selenium from landfill leachate by clay minerals. Soil Sci. Soc. Am. J. 41, 53–57.

Ganther, H.E., 1980. Interactions of vitamin E and selenium with mercury and silver. Micronutrient Interactions: Vitamins, Minerals and Hazardous Elements. Annals of New York Academy of Sciences, New York.

Girling, C.A., 1984. Selenium in agriculture and the environment. Agric. Ecosys. Environ. 11, 37–65.

Goldberg, S., Glaubig, R.A., 1985. Boron adsorption on aluminum and iron oxide minerals. Soil Sci. Soc. Am. J. 49, 1374–1379.

Goldberg, S., Forster, H.S., Heick, E.L., 1993. Boron adsorption mechanisms on oxides, clay-minerals, and soils inferred from ionic-strength effects. Soil Sci. Soc. Am. J. 57, 704–708.

Goldberg, S., Forster, H.S., Lesch, S.M., Heick, E.L., 1996. Influence of anion competition on boron. Soil Sci. 161 (2), 99–103.

Havercroft, J.M., Ward, N.I., 1991. Boron and other elements in relation to rheumatoid arthritis. In: Moncilovic, B. (Ed.), Trace Elements in Man and Animals 7. IMI, Zagreb.

Ishikawa, T., Nakamura, E., 1993. Boron isotope systematics of marine sediments. Earth Planet. Sci. Lett. 117, 567–580.

Kang, Y., Inoue, N., Rashid, M.M., Sakurai, K., 2002. Fixation of soluble selenium in contaminated soil by amorphous iron (hydr)oxide. Environ. Sci. 15, 173–182.

Keren, R., O'Connor, G.A., 1982. Effect of exchangeable ions and ionic strength on boron adsorption by montmorillonite and illite. Clay Clay Miner. 30, 341–346.

Keren, R., Sparks, D.L., 1994. Effects of pH and ionic strength on boron adsorption by pyrophyllite. Soil Sci. Soc. Am. J. 58, 1095–1100.

Levander, O.A., Deloach, D.P., Morris, V.C., Moser, P.B., 1983. Platelet glutathione peroxidase activity as an index of selenium states in rats. J. Nutr. 113, 55–63.

Lin, Z., Puls, R.W., 2000. Adsorption, desorption and oxidation of arsenic affected by clay minerals and aging process. Environ. Geol. 39, 753–759.

Majidi, A., Rahnemaie, R., Hassani, A., Malakouti, M.J., 2010. Adsorption and desorption processes of boron in calcareous soils. Chemosphere 80 (7), 733–739.

Manning, B.A., Fendorf, S.E., Goldberg, S., 1998. Surface structures and stability of arsenic(III) on goethite: spectroscopic evidence for inner sphere complexes. Environ. Sci. Technol. 32, 2383–2388.

Maraldi, T., Riccio, M., Zambonin, L., Vinceti, M., De Pol, A., Hakim, G., 2011. Low levels of selenium compounds are selectively toxic for a human neuron cell line through ROS/RNS increase and apoptotic process activation. Neurotoxicology 32, 180–187.

Mattigod, S.V., Frampton, J.A., Lim, C.H., 1985. Effect of ion-pair formation on boron adsorption by kaolinite. Clay Clay Miner. 33, 433–437.

Meng, X., Bang, S., Korfiatis, G.P., 2000. Effects of silicate, sulfate, and carbonate on arsenic removal by ferric chloride. Water Res. 34, 1255–1261.

Navarro-Alarcon, M., Cabrera-Vique, C., 2008. Selenium in food and the human body: a review. Sci. Total Environ. 400 (1–3), 115–141.

Nève, J., 1991. Physiological and nutritional importance of selenium. Experientia 47, 187–193.

Nielsen, F.H., 1994. Biochemical and physiologic consequences of boron deprivation in humans. Environ. Health Perspect. 7 (Suppl. 7), 59–63.

Nielsen, E.H., Hunt, C.D., Mullen, L.M., Hunt, J.R., 1987. Effect of dietary boron on mineral, estrogen and testosterone metabolism in post-menopausal women. FASEB J. 1, 394–397.

Nielsen, F.H., Mullen, L.M., Gallagher, S.K., 1990. Effect of boron depletion and repletion on blood indicators of Ca status in humans fed a low magnesium diet. J. Trace Elem. Exp. Med. 3, 45–54.

Parkhurst, D.L., Appelo, C.A.J., 1999. User's guide to PHREEQC (version 2) — a computer program for speciation, batch-reactions, one-dimensional transport, and inverse geochemical calculations. U.S. Department of the Interior and U.S. Geological Survey. Water Resour. Invest. Rep. 99, 4259.

Peak, D., Sparks, D.L., 2002. Mechanisms of selenate adsorption on iron oxides and hydroxides. Environ. Sci. Technol. 36, 1460–1466.

Pirajno, F., 2009. Hydrothermal Processes and Mineral Systems. Springer Science, The Netherlands.

Prezbindowski, D.R., Tapp, B., 1991. Dynamics of fluid inclusion alteration in sedimentary rocks: a review and discussion. J. Organic Geochem. 17 (2), 131–142.

Renard, F., Montes-Hernandez, G., Ruiz-Agudo, E., Putnis, C.V., 2013. Selenium incorporation into calcite and its effects on crystal growth: an atomic force microscopy study. Chem. Geol. 340, 151–161.

Rotruck, J.T., Pope, A.L., Ganther, H.E., Swanson, A.B., Hafeman, D.G., Hoekstra, W.G., 1973. Selenium: biochemical role as a component of glutathione peroxidase. Science 179, 588–590.

Shah, S.A., Vohora, S.B., 1990. Boron enhances anti-arthritic effects of garlic oil. Fitoterapia 61, 121–126.

Siegel, E., Wason, S., 1986. Boric acid toxicity. Pediatr. Clin. N. Am. 33, 363–367.

Smith, A.H., Hopenhayn-Rich, C., Bates, M.N., Goeden, H.M., Hertz-Picciotto, I., Duggan, H.M., Wood, R., Kosnett, M.J., Smith, M.T., 1992. Cancer risks from arsenic in drinking water. Environ. Health Perspect. 97, 259–267.

Spears, A., 1964. Boron in some British Carboniferous sedimentary rocks. Geochim. Cosmochim. Acta 20, 315–328.

Stoica, A., Pentecost, E., Martin, M.B., 2000. Effects of selenite on estrogen receptor-alpha expression and activity in MCF-7 breast cancer cells. J. Cell. Biochem. 79, 282–292.

Tabelin, C.B., Igarashi, T., 2009. Mechanisms of arsenic and lead release from hydrothermally altered rock. J. Hazard. Mater. 169, 980–990.

Tabelin, C.B., Igarashi, T., Tamoto, S., 2010. Factors affecting arsenic mobility from hydrothermally altered rock in impoundment-type in situ experiments. Min. Eng. 23, 238–248.

Tabelin, C.B., Igarashi, T., Takahashi, R., 2012a. The roles of pyrite and calcite in the mobilization of arsenic and lead from hydrothermally altered rocks excavated in Hokkaido, Japan. J. Geochem. Explor. 119, 17–31.
Tabelin, C.B., Igarashi, T., Takahashi, R., 2012b. Mobilization and speciation of arsenic from altered rock in laboratory column experiments under ambient conditions. Appl. Geochem. 27, 326–342.
Tabelin, C.B., Igarashi, T., Yoneda, T., 2012c. Mobilization and speciation of arsenic from hydrothermally altered rock containing calcite and pyrite under anoxic conditions. Appl. Geochem. 27, 2300–2314.
Tabelin, C.B., Igarashi, T., Yoneda, T., Tamamura, S., 2013. Utilization of natural and artificial adsorbents in the mitigation of arsenic leached from hydrothermally altered rock. Eng. Geol. 156, 58–67.
Tabelin, C.B., Igarashi, T., Arima, T., Sato, D., Tatsuhara, T., Tamoto, S., 2014a. Characterization and evaluation of arsenic and boron adsorption onto natural geologic materials, and their application in the disposal of excavated altered rock. Geoderma 213, 163–172.
Tabelin, C.B., Hashimoto, A., Igarashi, T., Yoneda, T., 2014b. Leaching of boron, arsenic and selenium from sedimentary rocks: I. Effects of contact time, mixing speed and liquid-to-solid ratio. Sci. Total Environ. 472, 620–629.
Tabelin, C.B., Hashimoto, A., Igarashi, T., Yoneda, T., 2014c. Leaching of boron, arsenic and selenium from sedimentary rocks: II. pH dependence, speciation and mechanisms of release. Sci. Total Environ. 473–474, 244–253.
Tatsuhara, T., Arima, T., Igarashi, T., Tabelin, C.B., 2012. Combined neutralization–adsorption system for the disposal of hydrothermally altered excavated rock producing acidic leachate with hazardous elements. Eng. Geol. 139–140, 76–84.
Travers, R.L., Rennie, G.C., Newnham, R.E., 1990. Boron and arthritis: the results of a double-blind pilot study. J. Nutr. Med. 1, 127–132.
Van Bochove, E., Prévost, D., Pelletier, F., 2000. Effects of freeze–thaw and soil structure on nitrous oxide produced in a clay soil. Soil Sci. Soc. Am. J. 84, 1638–1643.
Van Rij, A.M., Thomson, C.D., McKenzie, J.M., Robinson, M.E., 1979. Selenium deficiency in total parenteral nutrition. Am. J. Clin. Nutr. 32, 2076–2085.
Vinceti, M., Rovesti, S., Gabrielli, C., Marchesi, C., Bergomi, M., Martini, M., et al., 1995. Cancer mortality in a residential cohort exposed to environmental selenium through drinking water. J. Clin. Epidemiol. 48, 1091–1097.
Vinceti, M., Guidetti, D., Pinotti, M., Rovesti, S., Merlin, M., Vescovi, L., et al., 1996. Amyotrophic lateral sclerosis after long-term exposure to drinking water with high selenium content. Epidemiology 7, 529–532.
Vinceti, M., Rothman, K.J., Bergomi, M., Borciani, N., Serra, L., Vivoli, G., 1998. Excess melanoma incidence in a cohort exposed to high levels of environmental selenium. Cancer Epidemiol. Biomarkers Prev. 7, 853–856.
Vinceti, M., Crespi, C.M., Bonvicini, F., Malagoli, C., Ferrante, M., Marmiroli, S., Stranges, S., 2013. The need for a reassessment of the safe upper limit of selenium in drinking water. Sci. Total Environ. 443, 633–642.
Webster, J.G., 1999. Arsenic. In: Marshall, C.P., Fairbridge, R.W. (Eds.), Encyclopaedia of Geochemistry. Chapman Hall, London.
Wilkie, J.A., Hering, J.G., 1996. Adsorption of arsenic onto hydrous ferric oxide: Effects of adsorbate/adsorbent ratios and co-occurring solutes. Colloid Surf. A 107, 97–110.
Yang, G., Wang, S., Zhou, R., Sun, S., 1983. Endemic selenium intoxication of humans in China. Am. J. Clin. Nutr. 37, 872–881.